metals

Review

Slippage during High-Pressure Torsion: Accumulative High-Pressure Torsion—Overview of the Latest Results

Dmitriy V. Gunderov [1,2,*], Rashid N. Asfandiyarov [1,2], Vasily V. Astanin [2,3] and Alfred V. Sharafutdinov [2]

[1] Institute of Molecule and Crystal Physics of Ufa Federal Research Centre RAS, Prospekt Oktyabrya 151, 450075 Ufa, Russia
[2] Department of Materials Science and Physics of Metals, Ufa University of Science and Technology, 12 K. Marksa ul., 450008 Ufa, Russia
[3] Research Equipment Sharing Center "Nanotech", Ufa University of Science and Technology, 12 K. Marksa ul., 450008 Ufa, Russia
* Correspondence: dimagun@mail.ru

Abstract: This overview examines the results of a study of the effect of slippage in high-pressure torsion (HPT). A number of papers in this area and the works of the authors of this overview are considered. The authors used the method of the "joint HPT of the disk halves". This method is the simplest and most illustrative method for evaluating slippage during HPT. The authors used 10 and 20 mm diameter anvils, with a groove on the lower anvil and a calculated pressure of 6 GPa. In the case of the HPT of solid bulk metal glass (BMG), slippage starts at the early stages of HPT and is total. Slippage may also be significant at the early stages of the HPT of such metallic materials as Ti, Ni, Fe-0.1%C, and Zr-2.5%Nb. Slippage increases with the number of revolutions, n. There is no slippage at the initial stages of the HPT of copper. However, after HPT Cu n = 10, slippage can be total. Nevertheless, studies show that the structure of samples using HPT, obtained by the authors, is similar to the nanostructure observed by other authors after using HPT with similar materials. Thus, notwithstanding slippage during HPT, deformation during HPT still occurs, and nanostructure formation occurs. Therefore, the formation of a nanostructure in samples during HPT is not proof of the absence of slippage. The authors provide a possible explanation for this. The authors propose a new method—"accumulative high-pressure torsion"—to achieve a high strain in various materials. In this procedure, several cycles are repeated, according to the following scheme: "HPT for n = 1 or 2 turns of the anvil → cutting the specimen into pieces → unstacking the stacked pieces on the anvil and subsequent HPT for n = 1 or 2". Studies performed on a number of materials demonstrate that novel method transforms the structure more efficiently than regular HPT.

Keywords: high-pressure torsion; slippage; SPD processing; deformation; nanostructure

check for updates

Citation: Gunderov, D.V.; Asfandiyarov, R.N.; Astanin, V.V.; Sharafutdinov, A.V. Slippage during High-Pressure Torsion: Accumulative High-Pressure Torsion—Overview of the Latest Results. *Metals* **2023**, *13*, 1340. https://doi.org/10.3390/met13081340

Academic Editor: Marcello Cabibbo

Received: 22 June 2023
Revised: 12 July 2023
Accepted: 13 July 2023
Published: 26 July 2023

1. Introduction

High-pressure torsion (HPT) is the most powerful method to refine the structure of metallic materials [1–4]. In alloys, HPT can lead to phase transformations with the formations of metastable phases [1–3]. Some alloys may amorphize during HPT [5–7]. Nanostructured metals and alloys produced by HPT exhibit unique mechanical and physical properties that were not achievable in their coarse-grained counterparts [1–4,8–14]. In this regard, the topic of HPT is of great interest, and a large number of scientific groups are working on HPT. In the past 30 years, over 3000 papers, including famous reviews [1–3], have been published on the HPT of various metals and alloys.

Generally, the shear strain γ during high-pressure torsion can be estimated according to Equation (1) [2]:

$$\gamma = \frac{2\pi R n}{h}, \quad (1)$$

where n is the number of revolutions, R is the radius of the measuring point, and h is the thickness of the sample.

Various aspects of HPT have been considered in numerous articles [1–3,14–18]. In particular, the influence of HPT pressure, temperature, the design features of HPT anvils, etc., have been considered [1–3]. Traditionally, researchers have focused on the nanostructure and properties of various metals and alloys subjected to HPT. At the same time, it should be noted that researchers have used HPT with various applied pressures, numbers of revolutions, process temperatures, anvil rotation speeds, and anvil geometries, using metals with different contents of impurities [1–3]. This explains the fact that the results presented in different papers on the structure (grain size and microhardness) of the same metal or alloy in the HPT process can differ markedly, as in the case of the HPT of commercially pure (CP) Ti [9–15]. In [16], the homogeneity of deformation by high-pressure torsion was considered. In [17], the features of the mechanics of the flow of materials under high-pressure torsion were considered.

It is believed that HPT with a sufficiently large number of anvil revolutions ($n \geq 5$) leads to a very high degree of deformation of materials (according to Formula (1)), which ensures the formation of a nanostructure, as recorded in a huge number of works. (See, e.g., reviews [1–3] and articles [5–18].) It is considered that the force of friction between the surfaces of the sample and the anvils during rotation in the HPT process leads to a displacement of the upper part of the sample relative to the lower part of the sample. Equation (1) is true only in this case. However, it is known that in the HPT of some materials, "slippage" of the anvil over the surface of the sample is possible [3]. Slippage occurs if the functional force between the sample surface and the anvil surface becomes less than the pure shear limit (τ_s) of the sample. As a result, the actual shear strain γ_{real} may be much lower than expected. A number of works, in particular [3,19–24], are devoted to the slippage effect. Bridgman previously wrote that slippage is possible during HPT [4].

Thus, we can conclude that the slippage effect is not sufficiently studied. This topic is quite relevant, since the slippage effect can have a significant impact on the final result of the structure transformation and introduce ambiguity in the interpretation of the obtained results. This review focuses on the issue of slippage in HPT using an efficient methodology—"joint HPT of the disk halves"—to determine slippage.

2. Overview of Slippage in HPT

In [22–24], slippage during the HPT of bulk metallic glasses (BMGs) was investigated. In [22], the $Zr_{50}Cu_{40}Al_{10}$ bulk metallic glass was deformed using HPT with revolution numbers n = 1/4, 10, and 50 under a pressure of P = 5 GPa, at a revolution speed of 0.2 rpm. The anvils for the HPT process were "grooved" on the bottom surface and had corrugated surfaces to improve their grip during torsion. In [22], the following procedure was used to determine plastic strain and slippage during HPT (Figures 1 and 2): two semicircular specimens were prepared by cutting a single disk, and the two specimens were subjected to HPT. (This procedure is "the joint HPT of two disk halves" or "joint HPT.") After the "joint HPT" process, the top surfaces of the two semicircular disks were polished and etched [22]. As the interface between the two semicircular specimens was etched preferentially, the net shear displacement could be observed. Figure 2 displays the results of the experiments for the HPT with n = 5 [22]. The shear displacement degree (strain degree γ_{real}) can be evaluated according to the following equation (similar to Equation (1)):

$$\gamma_{real} = \theta R/h \text{ (if } R > 1 \text{ mm)}, \quad (2)$$

where θ is the shear angle (see Figure 2b).

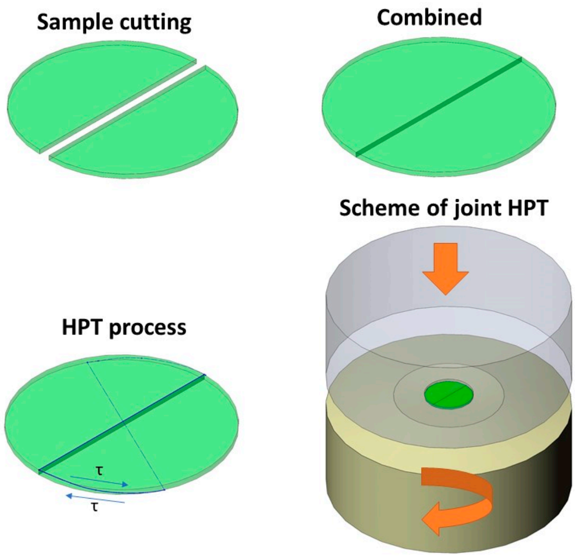

Figure 1. Procedure for observing the net shear strain γ_{real} introduced by the HPT process. The net strain introduced by the HPT process was calculated by Equation (2) using the shear angle τ (θ).

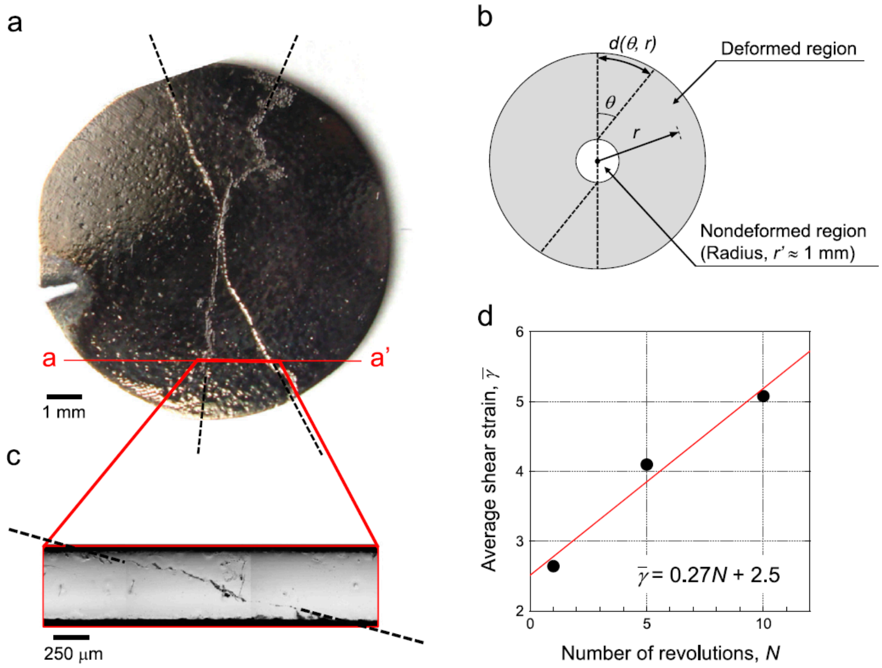

Figure 2. Results of the shear-displacement measurements performed on the HPT-processed disk: (**a**) image showing the net shear displacement introduced by the n = 5 HPT process; (**b**) definitions used for calculating the magnitude of the net shear strain, γ; (**c**) cross-sectional views of the shear displacement; (**d**) relation between the introduced shear strain, γ_{real}, and the number of revolutions, n, of the HPT process [22].

The torsional shear strain near the center of the disk ($0 < r < 1$ mm) was practically zero (the "non-deformed region"). In the region of the disk with $r > 1$ mm, the shear strain increased in proportion to r. As can be seen from Figure 2a, the shear strain after the HPT with n = 5 was only 3.5 (in the point r = 3 mm), whereas the shear strain calculated by Formula (1) was γ_{ideal} = 157 [22]. Thus, the γ_{real} for n = 5 was 45 times lower than the expected γ_{ideal}. Such a large difference between γ_{real} and γ_{ideal} was observed during the HPT at all the used n (Figure 2d) [22]. In [23], the effective strain during HPT was evaluated by inserting a small brass pin into a Zr-based BMG sample at some distance R from the rotation center and by examining brass deformation after torsion. The γ_{real} during the HPT with n = 10 at a radius of r = 3 mm from the center for the BMG samples was γ_{real} = 2.5 [23], whereas the calculated shear strain γ_{ideal} should be over 300.

Strain degree γ_{real} was evaluated during the HPT of the Zr-based BMG Vit105 sample using the improved method of "joint HPT of two disks halves" [22–24]. The Vit105 BMG sample (composition $Zr_{52.5}Cu_{17.9}Ni_{14.6}Al_{10}Ti_5$ at. %) in the form of a disk of 10 mm diameter and 0.8 mm thickness was used. This disk was cut into two halves, as shown in the scheme in Figure 1. The faces of both halves were polished and bonded with a thin layer of lacquer to prevent the consolidation of the halves [24,25]. As a result, the two halves of the disks after "joint HPT" were easily separated, and the γ_{real} could be evaluated from the geometry of the halves.

HPT was carried out using anvils with a diameter of 10 mm with a 0.5 mm deep groove, at a rotation speed of 1 or 0.5 rpm, under a calculated pressure of 6 GPa (the pressure calculation method is discussed below), at room temperature [25].

For comparison, halves of pure copper, a soft metal, were subjected to "joint HPT" for n = 1/4 revolution. according to a similar scheme. The shape of the Cu halves after "joint HPT" corresponded to the rotation angle of the anvils (Figure 3a), i.e., the strain γ_{real} introduced into the sample corresponded to Equation (1) [25].

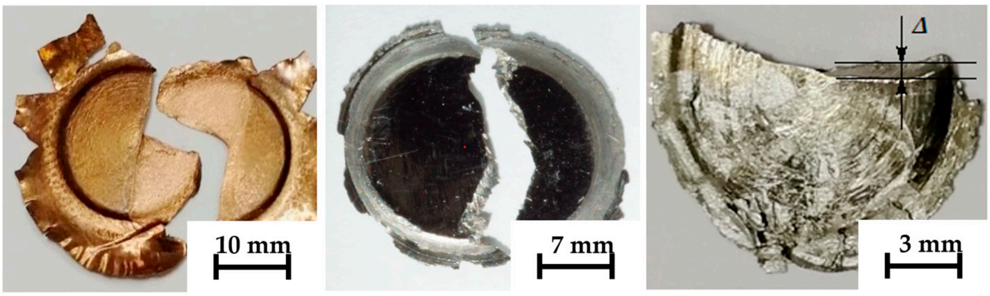

(**a**) (**b**) (**c**)

Figure 3. Images of the sample halves: (**a**) two halves of pure Cu after joint HPT for n = 1/4 revolutions; (**b**) two halves of the Vit105 BMG after joint HPT for n = 1 revolution; (**c**) a half of the BMG after joint HPT for n = 5 revolutions [25].

The view of the halves of the Vit105 BMG samples after the joint HPT at n = 1 revolution and n = 5 revolutions (Figure 3b,c) clearly indicates that the γ_{real} was significantly lower than the expected γ_{ideal}. The shear strain γ_{real} was calculated in [25], according to the following equation:

$$\gamma_{real} = \Delta/h, \tag{3}$$

where Δ is the displacement of the upper surface of a half (segment) with respect to the lower surface (Figure 3c) and h is the sample thickness. (Equation (3) is similar to Equations (1) and (2)).

Calculated according to Equation (3), the real strain in the point r = 2.5 mm after joint HPT for n = 5 was $\gamma_{real} \approx 1$, while the calculated $\gamma_{ideal} \approx 145$.

In the case of the Vit105 BMG halves after the joint HPT for n = 1, the picture was more complicated. In addition to the displacement of the upper surface of a segment with respect to the lower surface, a complex change in the shape of the halves was observed, which also indicated some deformation. The degree of strain, γ_{real}, was difficult to estimate in this experiment, but the γ_{real} was clearly lower than the expected γ_{ideal} ($\gamma_{ideal} \approx 25$ in the point r = 2.5 mm). Thus, during the HPT of the Zr-based BMG, slippage was very significant at both small and large degrees of HPT (n = 5). Significant slippage during the HPT of a Zr-based BMG [24] was explained by its high hardness and strength (HV > 4000 MPa, tensile strength > 1500 MPa). However, in [22–24], noticeable changes in the BMG structure were observed (i.e., change in the free volume ΔV as a result of the HPT), similar to those observed in the works of other authors who studied the HPT-treated amorphous alloys with a similar composition.

In addition, we were unable to find articles by other authors that evaluated slippage during the HPT of solid BMG and did not observe significant slippage. There were several papers, in particular [19,20], that investigated slippage during the HPT of crystalline metals and alloys. In [20], experiments were conducted to measure the extent of slippage occurring during the HPT of aluminum, copper, and iron. The upper and lower anvils of the rig were made from high-strength tool steel with nitride surfaces [20]. These two anvils with diameters of 10 mm contained, on their inner surfaces, groove depths of 0.25 mm. In [20], the method used for assessing slippage was the application of a scratch marker to the top and bottom surfaces of the disk subjected to HPT. The γ_{real} was estimated from the mutual displacement of the scratch-markers. The obtained γ_{real} (calculated by Equation (2) or (3)) was compared with the γ_{ideal} calculated by Equation (1) and the degree of slippage during HPT was estimated accordingly. However, during HPT with a relatively large number of anvil rotations ($n > 1$ or more), the marker scratches were erased from the surface of the samples under the action of HPT and this did not allow an estimation of the γ_{real}.

The results in [20] showed very little slippage for aluminum, slightly more slippage for copper, and significant slippage when iron was used. As can be seen, slippage increased with increasing metal strength. For all materials, the degree of slippage increased both at higher rotational speeds (1 rpm) and at lower imposed pressures. During the HPT of Fe at $n = 1/4$, with a rotational speed of 1 rpm, slippage was observed even at a pressure of $P = 5$ GPa. No slippage was detected during the HPT of all materials at a pressure of $P = 5$ GPa, $n = 1/4$, and a rotational speed of 0.5 rpm. However, slippage on Fe was not evaluated for HPT with n greater than 1/4. Slippage on copper was not evaluated for HPT with $n > 2$ [20]. However, it should be noted that slippage increased with an increasing number of revolutions, n, at HPT, and slippage increased with decreasing pressure to $P = 2$ GPa.

It should also be noted that the studies in [20] were performed on high-purity (99.99%) Al, high-purity (99.99%) Cu, and pure (99.96%) Fe. High-purity metals are known to have a low initial strength and little hardening by deformation. Consequently, slippage during their HPT can be much less than in the HPT of commercially pure metals (which are more hardened and more widely used in HPT experiments by various scientific groups).

In numerous studies (in particular [21]), the so called "pressure-dependent torque estimation" method was used to determine the slippage effect. That method consists of the following: A torque sensor is mounted on the HPT device [21] and a torque estimation curve (M) as a function of applied pressure is plotted on the HPT samples [21]. According to this technique, the curve M as a function of pressure (P) at pressures from $P = 0$ to a certain critical P_c runs in a straight line due to the slippage of the anvil on the sample. At some P_c, a "break" in the dependence $M(P)$ is observed. Such a break is thought to indicate that the frictional force $F\mu = \mu P$ in the anvil–sample contact becomes greater than the pure shear limit of the material ($F\mu > \tau_s$), and torsional deformation of the sample material begins [21]. However, this method is indirect, and the discontinuity of the $M(P)$ dependence in HPT process may be due to various factors that are difficult to account for. Direct methods, such as the "marker scratch on the upper and lower surfaces" method [20] or the "joint HPT of two halves" method [22], are more indicative and reliable. This method was previously used in one work to estimate slippage during the HPT of amorphous alloys [22]. However, this method, for some reason, was not previously used to estimate slippage at the HPT of crystalline metals and alloys.

The authors of the present paper have used the "joint HPT of two halves" method for the past 4 years to evaluate slippage on a number of metallic materials, see, e.g., [24–27]. It was shown that slippage on such a relatively mild material as copper was not so significant in the early stages of HPT [25,28]. However, during the HPT of such materials as mild steel (Fe-0.1% C), the Zr-1%Nb alloy, CP Ti, the β-Ti alloy, Ti-18Zr-15Nb, and the austenitic steel 316 (Fe–0.03C–17Cr–0.41Si–1.72Mn–0.01P–0.03S–12.9Ni–2.36Mo, wt.%) the slippage was revealed as follows [26–28]: samples of these materials received a certain degree of shear strain at the initial HPT stages, but significant slippage was observed already at the initial stages of HPT. However, the samples of these materials after HPT with $n > 5$, at further increase of n, did not lead to noticeable shear strain due to slippage.

In [28], slippage during the HPT of commercially pure Ti and Cu was additionally investigated. The results are detailed below.

In the experiments to evaluate slippage, typical technological regimes of HPT were used, as follows: anvils made of tool steel with a groove of 0.5 mm depth and a diameter of the working part of these anvils of 20 mm, no special surface roughness preparation, room temperature, and torsional speed 0.5 rpm. The initial samples for HPT had a surface after grinding on P1000 abrasive paper. These HPT modes and HPT equipment [29] were used in the works of specialists of the famous school of Professor R.Z. Valiev from former Ufa State Aviation Technical University (now Ufa University of Science and Technology).

Experiment I. Figure 4a shows that the relative shift of the upper and lower surfaces of the Ti halves was quite large and the degree of γ_{real} was close to the γ_{ideal} expected for HPT with $n = 1/4$. Thus, at this HPT regime (flat anvils, $n = 1/4$, $P = 6$ GPa), slippage was insignificant.

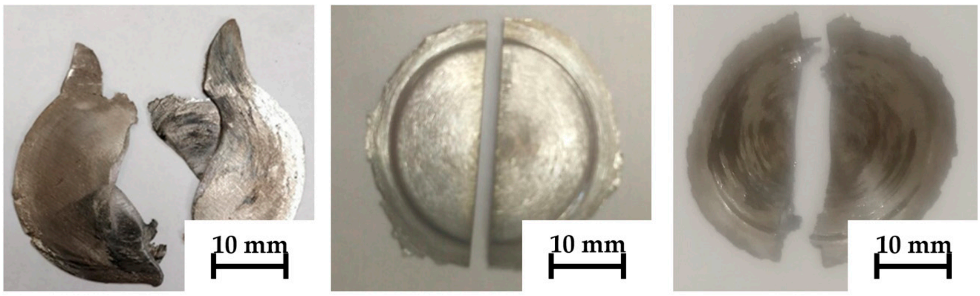

(**a**) (**b**) (**c**)

Figure 4. (**a**) Ti halves after joint HPT $n = 1/4$ on flat anvils; (**b**) Ti disk after HPT $n = 5$ cut for joint HPT; (**c**) the same halves after subsequent joint HPT $n = 1$ ($n = 5 + 1$) [28].

However, in the case of the joint HPT of the Ti disk halves on anvils 20 mm in diameter having a groove with a depth of $h = 0.5$ mm ($P = 6$ GPa, room temperature), noticeable slippage already occurred at the initial stage of HPT—$n = 1/4$ [28].

Experiment II [28]. The whole Ti disk was first subjected to HPT with $n = 5$, then the resulting HPT disk was cut into two halves (Figure 4b). These halves were subjected to joint HPT with $n = 1$ (Figure 4c). The view of the sample was almost unchanged (Figure 4c); there was no displacement of the upper and lower surfaces of the halves in most of the sample. Thus, after the preliminary HPT with $n = 5$, complete slippage was observed on the Ti specimen.

As shown above (Figure 4a), the slippage effect was not so significant in the initial stages ($n = 1/4$) of the HPT of Cu [28]. However, we decided to investigate how the slippage on Cu changes as the number of HPT revolutions increases.

Experiment III [28]. The whole CP Cu disk was first subjected to HPT with $n = 5$, then the resulting HPT disk was cut into two halves (Figure 5a). The resulting halves were subjected to joint HPT with $n = 1/4$. The change in the shape of the lower part of the sample (Figure 5b) indicated significant deformation (due to the displacement of the upper and lower surfaces). However, the strain γ_{real} in the upper part of the sample was clearly lower than the expected γ_{ideal}. Thus, after preliminary HPT with $n = 5$, slippage was significant even on relatively mild Cu. Moreover, the degree of deformation was not the same in different parts of the sample.

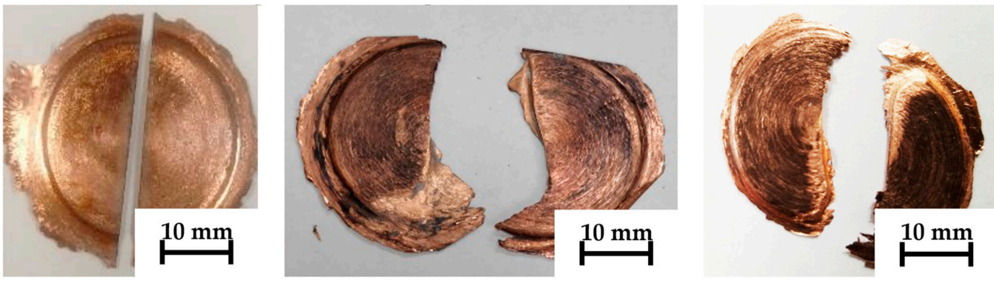

(**a**) (**b**) (**c**)

Figure 5. (**a**) Copper disk after HPT with $n = 5$ cut into halves; (**b**) the same halves after subsequent joint HPT $n = 1/4$ [28]; (**c**) copper sample after HPT $n = 10$ cut into halves, and the same halves after subsequent joint HPT $n = 1$ (new result).

Experiment IV. The whole CP Cu disk at the first stage was subjected to HPT with $n = 10$, then the resulting disk was cut into two halves and the resulting halves were subjected to joint HPT with $n = 1$. The shape of the halves nearly did not change (Figure 5c). Thus, slippage in Cu after the preliminary HPT with $n = 10$ became total.

Thus, recent studies demonstrated that during the HPT of such materials as mild steel (Fe-0.1% C) [27], the Zr-1%Nb alloy [26], and CP Ti [28], slippage is more or less observed at the initial stage of HPT ($n = 1/4$), while after HPT, with a larger number of revolutions ($n = 5$), slippage becomes total and shear strain does not increase with n.

We investigated the structure of HPT-treated samples through regimes in which slippage was detected [26–28]. The study showed that such HPT with $n = 5$ or $n = 10$ resulted in the formation of a nanostructured state in Zr-1%Nb alloy [26], Fe-0.1%C steel [27], CP Ti [28], and 316 steel similar to that observed by other authors in comparable materials after HPT [29–37]. HPT-induced ω-phase formation was observed in Zr-1%Nb alloy [26] and CP Ti [28], as previously observed in [10–14,32–34]. Thus, the structure refinement of the selected materials occurred in the HPT process, despite the slippage during HPT in our experiments in the selected modes.

Thus, Figure 6 shows the pattern of X-ray diffraction of CP-Ti in the initial state and after HPT $n = 10$ [28]. (HPT modes corresponded to those described above for HPT on anvils with a diameter of 20 with a groove). X-ray diffraction analysis (Figure 6) showed that, as a result of buildup (despite fixed slip), microdistortions grew and the sizes of coherent scattering regions decreased, compared to the initial state [28]. Microdistortions grew and the sizes of coherent scattering regions reached values close to similar parameters achieved by HPT CP Ti in the works of other authors [10–14]. In addition, the appearance of ω-phase, due to $\alpha \rightarrow \omega$ transition after HPT, was observed [28], as shown earlier [12,13].

Analysis of the TEM of Ti after HPT (Figure 7) showed nanostructure formation with high dislocation density, and internal stresses and a grain size of about 100 nm. The observed structure was close to that of HPT CP Ti noted of other authors [11–13]. Thus, we first recorded the slippage during build-up for the used CP Ti modes. Second, all structural transformations observed by us after HPT were similar to those noted by other authors in HPT CP Ti.

The most important issue to explain slippage during HPT is the force of friction between the anvil and the specimen surface. There are three main types of external friction: resting, sliding, and rolling. Generally, when considering contact friction in metal forming methods, the focus is on sliding friction, and in most machining schemes (drawing, pressing, etc.) the external friction forces play a negative role. However, in HPT, the external friction forces should provide for the capture of the workpiece and the transfer of energy required for the plastic deformation of the metal by the anvil, by analogy with the capture of the workpiece during rolling [38]. That is, the forces of external friction in the contact zone between the anvil and the workpiece during the HPT process provide rotation of the upper part of the sample relative to the lower part and, accordingly, shear deformation in the sample. However, as mentioned above, it is known that during the HPT of high-strength materials, "slippage" of the anvil on the surface of the sample is possible [3]. Thus, the external friction and its magnitude determine the fundamental possibility of the HPT process, as well as the probability of anvil slippage relative to the workpiece.

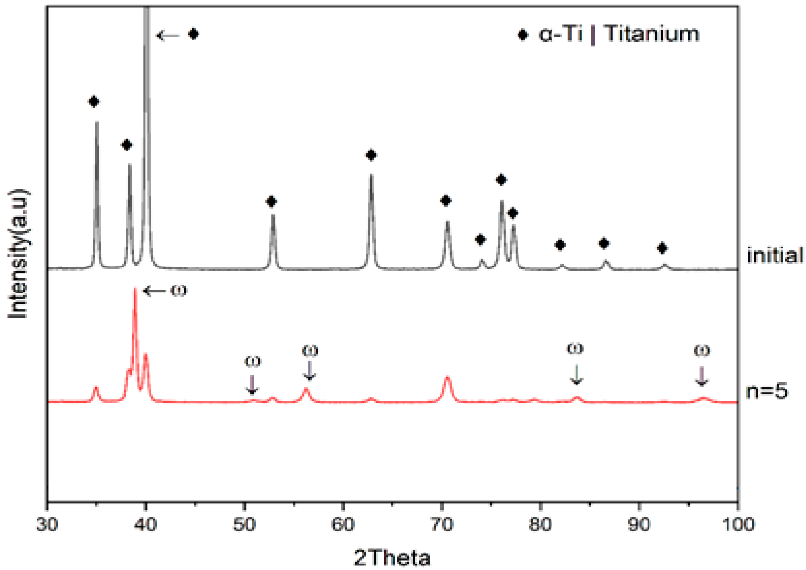

Figure 6. XRD date for CP-Ti in the initial state and after HPT n = 5 [28].

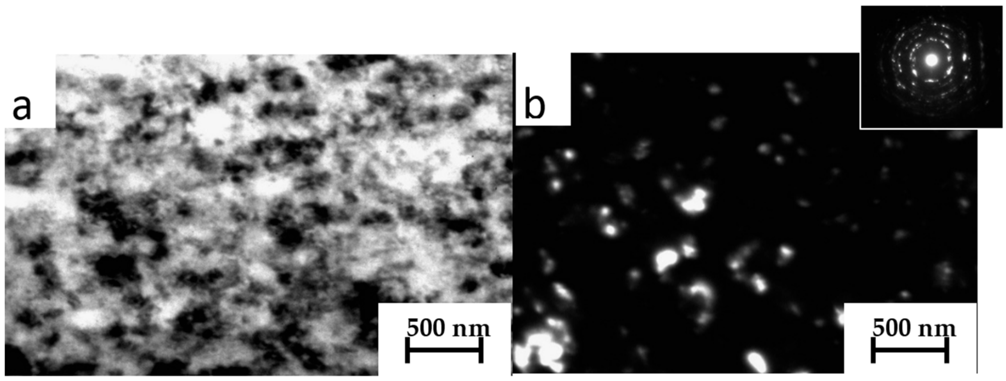

Figure 7. Structure of Ti after HPT n = 10: (**a**) bright field; (**b**) dark field with an electron diffraction pattern [28].

A detailed analysis of the above shows that the torsion process, depending on the presence of "slippage", should be characterized by two types of friction—sliding and resting.

In the case of "slippage", sliding friction will prevail, which is characterized by the fact that the surface points of the workpiece move tangentially to the surface of the anvil, and the shear stresses τ_x arising in the contact obey the Amonton–Coulomb law:

$$\tau_x = \mu\, P_x, \tag{4}$$

where μ is the coefficient of friction and P_x is the normal contact stress.

However, to exclude "slippage", it is necessary to ensure certain conditions so that the peripheral speed of the anvil is equal to the speed of movement of the surface layer of the workpiece, in which case the friction stresses increase sharply, reaching their maximum value — pure shear resistance τ_s. The anvil and the workpiece begin to move together, in which case "sticking" is observed. The term "sticking" characterizes the section of the contact surface where there is no relative sliding of the anvil and workpiece contact surfaces, i.e., the external sliding friction becomes internal, and the contact surface begins to be subject to resting friction. The magnitude of friction forces and stresses in the "sticking" zone does not obey the law (1) and does not depend on factors affecting the friction coefficient—surface roughness, lubrication, etc.—but depends on the resistance to pure material shear [38]:

$$\tau_x = \tau_s \tag{5}$$

The next factor to be analyzed is the pressure applied during HPT [15,23]. This pressure can be calculated by the following formula:

$$P = F/S \tag{6}$$

where F is the force and S is the area on which the force is applied.

When calculating the area S, researchers usually take the area of the anvil. However, in reality, the contact area of the anvil with the material must be larger than that of the working part of the anvil alone, taking into account the geometric imperfections of the tooling and flash, which results in a lower final specific pressure [28]. It was shown in [28] that the force applied at HPT was F = 2000 kN and the diameter of the anvil working part d = 20 mm; hence, the anvil area was S = 314 mm^2, and for this area the calculated specific pressure was P = 6 GPa. However, considering the bursting of the material, the diameter of the sample after HPT was d = 25 mm. Consequently, the real sample area S = 490 mm^2. If we assume that the contact area of the sample with the anvil was S = 490 mm^2, the real specific pressure would have been much lower, about 4 GPa.

Based on the above, consider calculating the friction force between the anvil and the workpiece. Anvils for HPT are usually made of high-strength tool steel. The coefficient of friction in the steel–steel pair is μ = 0.15 [39]. The yield strength of annealed Fe-1%C steel is about 500 MPa. However, it is known that during HPT deformation, steel hardens in the early stages of HPT, and at HPT $n > 1$, its yield strength increases to 1500 MPa and more [29–31]. It is known that for many metals and alloys, the pure shear resistance is $\tau_s = 0.58\sigma_{ys}$, where σ_{ys} is the yield strength of the material.

As shown above, condition (2) must be satisfied to eliminate slippage during HPT torsional deformation. Taking μ = 0.15, we determined that the torsional strain pressure under the HPT scheme of the original steel must be at least 1.95 GPa, and the strain pressure of the steel hardened in the first stages of HPT must be at least 5.8 GPa. It should be noted that in most works e.g., [29–31] on HPT steel, the specified applied pressure was 6 GPa or less. Taking into account the actual contact area, the actual value of specific pressure as 4 GPa or less. This explains the fact that [27] observed total slippage during HPT of low-carbon Fe-1%C steel with an increasing degree of HPT.

In the case of HPT Ti, a sliding friction coefficient of 0.4 in the steel–titanium pair must be used to analyze the slippage effect [39]. Hence, taking into account the real area, the required pressure was P = 2.75 GPa for HPT of coarse-grained Ti, which was quite feasible, but for nanostructured titanium, taking into account the real area, the required pressure was P = 7.8 GPa. A, slippage was observed after the first steps of HPT [28].

In addition, it should be noted that during HPT, material from the center of the sample flows sideways, out from under the anvils, in the form of burrs. Accordingly, the thickness of the sample becomes smaller with an increasing number of revolutions, n. During HPT, relatively strong materials wear down the anvils and a crater (depression) appears on them. Accordingly, as n increases during HPT and the thickness of the sample in the groove decreases, the area of the anvils at their edge (the burr area) experiences more and more pressure. Meanwhile, the pressure in the deformation zone of the sample decreases and becomes lower than the critical P_c. As a result, slippage is activated. Kuhlmann-Wilsdorf et al. suggested that there is also a certain relationship between decreasing specimen thickness and slippage during HPT [21].

The slippage effect depends in a complex way on several HPT parameters, including pressure, anvil design, anvil roughness, rotational speed, and other parameters. Other experts may argue that the slippage we observed were isolated cases related to shortcomings of the used devices or HPT regimes. Nevertheless, the issue of slippage during HPT remains relevant. As mentioned above, the studies [22–28,40], which demonstrated slippage on a number of materials, were performed using the HPT process modes that were traditional for the team. We used the HPT device from Ufa State Aviation Technical University (USATU, renamed Ufa University of Science and Technology). Using the same HPT device and modes, USATU staff have conducted research over the past 20 years, which resulted in hundreds of papers. All of the papers demonstrate significant grain refinement in various metallic materials during the HPT process. As we have shown, our most interesting result is that it is possible that grain refinement occurred in spite of slippage during HPT. Our results indicate that the refinement of the structure and the formation of a nanostructural state as a result of HPT is not proof of the absence of slippage.

The works of other research groups evaluating, by direct methods, the slippage during HPT with $n > 5$ of such materials as CP Ti, Ti alloys, steels, and other relatively strong metallic materials have not been found. Works are known [22,23] that demonstrate strong slippage from the initial stages of HPT in BMGs. We believe that the estimation of torque as a function of pressure is indirect and does not prove the absence of slippage.

In 2023, an article [41] appeared detailing the possible effects of slippage in terms of the mechanics of a deformable body, including the peculiarities of the action of frictional forces during HPT. This work confirmed our results.

As stated, readers may object that the HPT slippage observed in our experiment is the result of violations of the HPT parameters.

However, we believe that our result requires attention. Other HPT specialists can refute our results by using the "joint HPT disk halves" method to estimate slippage. This method is the simplest and most obvious method for evaluating HPT slippage. Other HPT specialists can use this method to carry out an experiment on their equipment and show that they have no HPT slippage. Alternatively, it may turn out that HPT slippage is just as significant on their equipment, and the effect of HPT slippage requires additional detailed investigation.

As shown above, despite significant slippage, the structure of materials during HPT refines to a nanostructured state [25–28,40]. How can deformation accumulate in the sample during HPT if slippage occurs? One possible explanation is that the planes of the upper and lower anvils are tilted relative to each other by a small degree [28]. Figure 8a shows an image of a titanium disk sample after HPT. The sample (diameter 20 mm) has a non-uniform thickness h. At one edge, h is 0.71 mm and at the other edge it is 0.66 mm [28]. This can be explained by the fact that the upper and lower anvils are inclined relative to each other at an angle of $\approx 0.15°$. In this case, when the anvils rotate relative to each other, the sample material under pressure of 6 GPa flows from one zone under the anvils to the other. As a result, the material undergoes deformation [28].

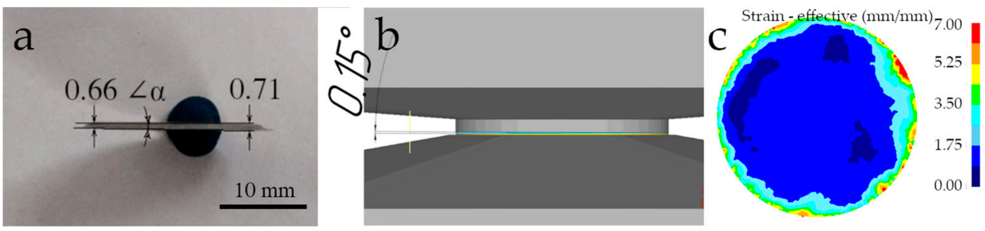

Figure 8. (**a**) Cross-section of the sample after HPT with a height difference forming an angle = 0.15°; (**b**) scheme of the HPT, in which the anvils are at an angle of 0.15° to each other; (**c**) distribution of accumulated strain intensity after five revolutions of HPT [28].

The case with this deformation pattern was reproduced using a finite-element computer simulation using the Deform 3D software package (Figure 8b) [28]. As in the real experiment, a CP Ti sample with d = 20 mm and h = 0.6 mm was taken for modeling. The material was assumed to be plastic and isotropic; it had no initial stresses and strains, and the anvil was specified as an absolutely rigid body.

Three-dimensional solid models of the sample and anvil were created using the CAD system KOMPAS-3D. A finite element grid of tetrahedrons was created. The number of finite elements was selected on the basis of preliminary calculations and was 75,000 [28]. The friction coefficients μ between the sample and the anvil were assumed to be 0.05. Total torsional slippage will occur at this small μ and the torsional strain does not contribute to the total strain. The anvil rotation speed was chosen to be constant and equal to 1 rpm. Simulations were performed with a constant time step of 0.1 s. The method of conjugate gradients was used. The finite-element model described the motion of a continuous medium based on the Lagrangian approach [28].

Figure 8c shows the distribution of the strain intensity (e_i) after five revolutions of the HPT. The data obtained show that even for the case μ = 0.05 (assuming that the anvil slides on the surface of the workpiece), at HPT n = 5, the value of the accumulated strain intensity changes from $e \approx 0.9$ at the disk center to $e \approx 7$ at the disk edges. This shows that a scheme in which "the upper and lower anvils are tilted relative to each other at an angle of about 0.15° leads to the accumulation of a significant amount of strain, which, taking into account the applied pressure of 6 GPa, can lead to the formation of nanostructure.

3. Short Overview of Accumulative HPT

The "slippage" effect [4] limits the possibility of achieving very high strains in relatively strong metallic materials. Therefore, in [42], we proposed a new technique, "accumulation torsion under high pressure" (ACC HPT), which allows achieving higher strains in such materials than conventional HPT. In the accumulative HPT process [42–45], the sample is subjected to several deformation cycles, according to the following scheme: "HPT for n = 1 or 2 turns of the anvil → cutting the specimen into pieces → unstacking the stacked pieces on the anvil and subsequent HPT for n = 1 or 2". Such cycles are repeated several times. In the final stage, the stacked segments are subjected to HPT with a large number of rotations ($n \geq 3$), which leads to the consolidation of the sample into a monolithic disk (similar to what is observed during HPT consolidation of amorphous ribbons and powders [1,2]). The proposed accumulative HPT method has some similarities with the well-known accumulative roll bonding method [46–48], but it also has certain advantages [42–45]. In addition, the proposed accumulative HPT method has some similarities with the high speed high pressure torsion (HSHPT) method used in [49]. The authors of [49] used the HSHPT method with a similar approach: after the HSHPT cycle, the Ni–Ti composite sample was cut into two parts, the parts were stacked on top of each other, and a new HSHPT cycle was performed. These cycles of HSHPT cutting of samples were repeated 16 times; as a result, the authors managed to obtain a fairly homogeneous Ni–Ti composite [49].

In [42,43], the HPT ACC was applied to Zr-based BMG Vit105 and a Zr-based intermetallide. In [44,45], ACC HPT was applied to Zr-1%Nb alloy, Fe-0.1%C steel, 316 austenitic steel, and β-Ti alloy. It was shown that ACC HPT more effectively improves the structure of crystalline materials [44,45] and more effectively transforms the structure of amorphous materials [42,43] than conventional HPT.

It is of great interest to obtain composites and hybrid materials using HPT [50–53]. However, with a limited number of rotations ($n \leq 5$) in the center of the HPT samples in works [50–53], heterogeneously mixed metal layers were observed.

In [54], cumulative high-pressure torsion was applied to obtain a Cu–Al metal matrix composite (in this case, the advantage of ACC HPT was most obvious). Disks of commercially pure copper and aluminum with a diameter of 20 mm and a thickness of 0.5 mm were stacked with alternating Cu-Al-Cu layers and deformed by two methods: conventional HPT and ACC HPT [54]. Conventional HPT and ACC HPT were performed at 6 GPa, room temperature, and 1 rpm. Anvils with a diameter of 20 mm and a groove depth of 0.5 mm were used for deformation.

Conventional HPT was performed with n = 10 rotations.

ACC HPT was performed as follows:

(Cycle 1) Cu–Al–Cu disks were sequentially stacked on top of each other on anvils. HPT n = 2 (two revolutions) at 6 GPa was performed. After HPT n = 2, a solid sample disk with a diameter of 20 mm and a thickness of about 0.7 mm (which is close to a groove depth of 0.5 mm) was obtained.

(Cycle 2) The resulting disk was cut into two halves. The halves were stacked on top of each other on the anvil. The thickness of the stacked halves was 1.4 mm. First, pressure up to 6 GPa was applied to the pile. This pressure exceeded the yield strength of the deformed material. Then, HPT n = 2 was carried out. Under the action of pressure and HPT n = 2, deformation took place, and the pile of halves again took the form of a disk with the thickness of 0.7 mm and diameter of 20 mm. From there, the material obtained about 50% tensile strain and some torsional strain (which was difficult to estimate).

(Cycle 3) The sample disk after 2 cycles, which was about 0.7 mm thick, was cut into two halves. The halves were stacked one on the other on the anvil. The pressure was applied up to 6 GPa. HPT n = 2 was performed. The material obtained about 50% tensile strain and some torsional strain.

(Cycle 4) The sample, an 0.7 mm thick disk, was cut into two halves again after 3 cycles. The halves were stacked on each other on the anvil. Pressure up to 6 MPa was applied. HPT n = 4 as performed (a higher number of turns n at the last stage of the ACC HPT allowed a stronger and more monolithic sample to be obtained). The material again received about 50% settling deformation and some torsional deformation. In total, the number of anvil rotations during the ACC HPT was $n\Sigma$ = 10. In each of the three stack settling cycles described above, the material received 50% of the settling deformation, which were added together. The total settling deformation of the material was about 90%. This settling deformation was significant and led to a refinement of the structure. In each cycle, the material also underwent torsional deformation, which was difficult to estimate. Another point to consider is that, as mentioned above, the torsional strain/slip rate depends on the height of the sample (elevation of the sample over the groove) [41]. If we perform the cycle "cut the specimen into two halves, with the halves laid on the anvil, pressure to 6 GPa, and HPT n = 2 at the HPT stage, the height of the halves (of the specimen) was noticeably greater than the depth of the groove. This can provide, in cycles, a total torsional strain greater than the normal HPT n = 10 in continuous mode. With the normal HPT n = 10 in continuous mode at larger n (n > 5), the sample thickness becomes minimal, close to the groove depth, which can lead to an increase in slippage.

The results of HPT on the composite clearly indicated the advantage of ACC HPT over conventional HPT. SEM images of cross sections of Cu–Al–Cu composites after conventional HPT are shown in Figure 9. Three characteristic Cu–Al–Cu layers (Cu — light layers, Al — dark layer) are clearly visible in the central parts and in the 1/2 R region of the sample (Figure 9a,d). Thus, the Cu and Al layers in these regions of the sample did not mix, even after traditional HPT with n = 10. At the edge of the sample, the Cu and Al layers mixed better, and curved lamellae were formed (Figure 9b). This behavior of the samples was typical for metal matrix composites obtained by HPT for Al–Cu bimetallic systems [55–57] and Al–Mg [58].

The pattern after ACC HPT (Figure 10) was significantly different than that after conventional HPT [54]. A well-mixed structure was observed in the central part of the sample after ACC HPT, where thin lamellae of Cu and Al were formed (Figure 10d) [54]. The microstructure with such vortex-folded lamellae was analyzed in [59]. The mixing process was intensified in the center of the sample, and the lamellae were more uniformly distributed along the sample. The microstructure at the edge of the sample (Figure 10b) was similar to the microstructure in the center. In contrast to conventional HPT, where mixing was observed at the edge of the sample, ACC HPT resulted in the mixing of the structure throughout the entire sample volume [54].

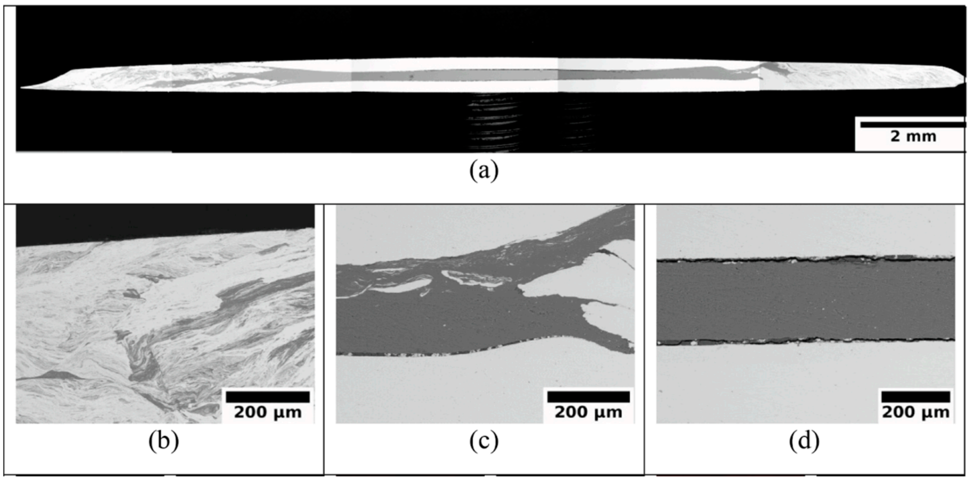

Figure 9. Cross-section of the Cu–Al–Cu metal matrix composite after conventional HPT at a lower magnification (**a**) and the zone of the edge (**b**), mid-radius (**c**), and center (**d**) at a higher magnification [54].

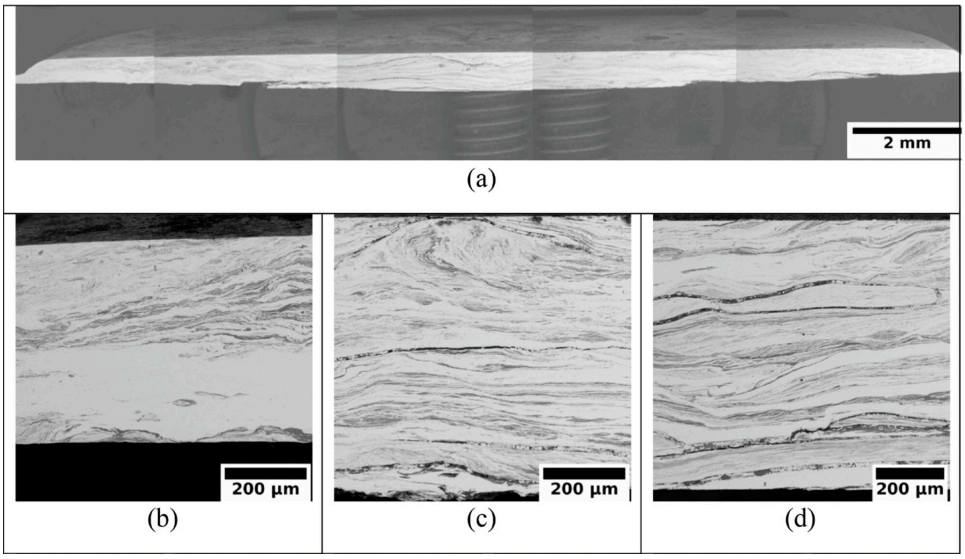

Figure 10. Cross-section of the Cu–Al–Cu metal matrix composite after accumulative HPT at a lower magnification (**a**) and the zone of the edge (**b**), mid-radius (**c**), and center (**d**) at a higher magnification [54].

XRD of Cu–Al–Cu composites after conventional HPT showed only Cu and Al diffraction maxima. The mixing processes in this sample were slow [54]. Al–Cu and Cu–Al solid solutions were formed after the accumulation HPT, according to XRD data.

The results presented in this study show that the accumulation of HPT is an effective method of mixing the structure of dissimilar metals and achieving structure transformation.

4. Conclusions

The phenomenon of slippage during high-pressure torsion deformation of various metallic materials was investigated. The works of several research groups on this topic were analyzed.

Numerous studies have used the "pressure-dependent torque estimation" method to determine the presence of the slippage effect. However, this method is indirect, and the discontinuity of the M(p) relationship at HPT can be explained not only by replacing slip with material flow, but also by other factors that are difficult to account for. Direct methods, such as the "marker scratch on the top and bottom surfaces" method, are more indicative and reliable. However, when conducting HPT with a relatively high number of anvil rotations ($n > 1$ or more), the marker scratches are erased from the surface of the samples under the action of HPT, which makes it impossible to estimate the real strain.

Previous works [22,23] demonstrated a strong slippage from the initial HPT stages to HPT with $n = 10$ when processing BMGs. In [22], the "joint HPT of two disk halves" method was used to estimate slippage. The "joint HPT" method is simple and illustrative, and can be used for HPT with a large number of rotations.

Studies of the authors of papers [26–28], using the "joint HPT" method, showed that during HPT of such materials as low-carbon steel, Zr-1%Nb alloy, and CP Ti, slippage is more or less already observed at the initial stage of HPT ($n = 1/4$), and after HPT with a greater number of revolutions ($n = 5$), slippage becomes complete. At the same time, HPT leads to the formation of a nanostructured state similar to that observed by other authors in similar materials after HPT. Consequently, the formation of nanostructured states and specific phase transformations during HPT are not indicative of the absence of slippage during HPT.

The authors proposed one of the possible explanations for the observed structure refinement in the sample during HPT, despite slippage: i.e., the presence of an inclination of the planes of the upper and lower anvil relative to each other by a small degree, which leads to the accumulation of deformation in the sample.

The authors proposed a new technique, "accumulative high-pressure torsion" (ACC HPT), which, as has been demonstrated in several papers, facilitates initially higher deformations and a stronger structural transformation in metallic materials than conventional HPT.

Author Contributions: Conceptualization, D.V.G.; methodology, V.V.A.; software, R.N.A.; formal analysis, D.V.G.; investigation, D.V.G. and A.V.S.; writing—original draft, D.V.G.; writing—review and editing, V.V.A. and R.N.A.; supervision, D.V.G.; project administration, D.V.G. All authors have read and agreed to the published version of the manuscript.

Funding: This research was funded by the Russian Science Foundation under project No. 22-19-00347.

Data Availability Statement: All data generated or analyzed during this study are included in the published article and are available from the corresponding authors upon request.

Acknowledgments: The authors are grateful to the personnel of the Research Equipment Sharing Center "Nanotech" of Ufa University of Science and Technology for their assistance with instrumental analysis. We also thank Sofia Gunderova for her help in preparing this paper.

Conflicts of Interest: The authors declare no conflict of interest.

References

1. Zhilyaev, A.P.; Langdon, T.G. Using high-pressure torsion for metal processing: Fundamentals and applications. *Prog. Mater. Sci.* **2008**, *53*, 893–979. [CrossRef]
2. Valiev, R.Z.; Zhilyaev, A.P.; Langdon, T.G. *Bulk Nanostructured Materials*; John Wiley & Sons, Inc.: Hoboken, NJ, USA, 2013; ISBN 9781118742679. [CrossRef]
3. Edalati, K.; Horita, Z. A review on high-pressure torsion (HPT) from 1935 to 1988. *Mater. Sci. Eng. A* **2016**, *652*, 325–352. [CrossRef]
4. Bridgman, P.W. Effects of High Shearing Stress Combined with High Hydrostatic Pressure. *Phys. Rev.* **1935**, *48*, 825–847. [CrossRef]
5. Popov, A.G.; Gaviko, V.S.; Shchegoleva, N.N.; Puzanova, T.Z.; Ermolenko, A.S.; Stolyarov, V.V.; Gunderov, D.V.; Raab, G.I.; Valiev, R.Z. Severe plastic deformation of R-Fe-B (R = Pr or Nd) hard magnetic alloys. *Phys. Met. Metallogr.* **2002**, *94*, S75–S81.
6. Waitz, T.; Kazyhanov, V.; Karnthaler, H.P. Martensitic phase transformations in nanocrystalline NiTi studied by TEM. *Acta Mater.* **2004**, *52*, 137–147. [CrossRef]
7. Sergueeva, A.V.; Song, C.; Valiev, R.Z.; Mukherjee, A.K. Structure and properties of amorphous and nanocrystalline TiNi prepared by severe plastic deformation and annealing. *Mater. Sci. Eng.* **2003**, *339*, 159–165. [CrossRef]
8. Gunderov, D.; Lukyanov, A.; Prokofiev, E.; Kilmametov, A.; Pushin, V.; Valiev, R. Mechanical properties and martensitic transformations in nanocrystalline $Ti_{49.4}Ni_{50.6}$ alloy produced by high-pressure torsion. *Mater. Sci. Eng. A* **2009**, *503*, 75–77. [CrossRef]
9. Popov, A.A.; Pyshmintsev, I.Y.; Demakov, S.L.; Illarionov, A.G.; Lowe, T.C.; Sergeyeva, A.V.; Valiev, R.Z. Structural and mechanical properties of nanocrystalline titanium processed by severe plastic deformation. *Scr. Mater.* **1997**, *37*, 1089–1094. [CrossRef]

10. Islamgaliev, R.K.; Kazyhanov, V.U.; Shestakova, L.O.; Sharafutdinov, A.V.; Valiev, R.Z. Microstructure and mechanical properties of titanium (Grade 4) processed by high-pressure torsion. *Mater. Sci. Eng. A* **2008**, *493*, 190–194. [CrossRef]
11. Valiev, R.Z.; Sergueeva, A.V.; Mukherjee, A.K. The effect of annealing on tensile deformation behavior of nanostructured SPD titanium. *Scr. Mater.* **2003**, *49*, 669–674. [CrossRef]
12. Stolyarov, V.; Zhu, Y.; Lowe, T.; Islamgaliev, R.; Valiev, R. A two step SPD processing of ultrafine-grained titanium. *Nanostruct. Mater.* **1999**, *11*, 947–954. [CrossRef]
13. Kilmametov, A.R.; Khristoforov, A.V.; Wilde, G.; Valiev, R.Z. X-ray studies of nanostructured metals processed by severe plastic deformation. *Z. Krist.* **2007**, *2007*, 339–344. [CrossRef]
14. Edalati, K.; Matsubara, E.; Horita, Z. Processing Pure Ti by High-Pressure Torsion in Wide Ranges of Pressures and Strain. *Metall. Mater. Trans. A* **2009**, *40*, 2079–2086. [CrossRef]
15. Shirooyeh, M.; Xu, J.; Langdon, T.G. Microhardness evolution and mechanical characteristics of commercial purity titanium processed by high-pressure torsion. *Mater. Sci. Eng. A* **2014**, *614*, 223–231. [CrossRef]
16. Vorhauer, A.; Pippan, R. On the homogeneity of deformation by high pressure torsion. *Scr. Mater.* **2004**, *51*, 921–925. [CrossRef]
17. Estrin, Y.; Molotovnikov, A.; Davies, C.; Lapovok, R. Strain gradient plasticity modelling of high-pressure torsion. *J. Mech. Phys. Solids* **2008**, *56*, 1186–1202. [CrossRef]
18. Estrin, Y.; Vinogradov, A. Extreme grain refinement by severe plastic deformation: A wealth of challenging science. *Acta Mater.* **2013**, *61*, 782–817. [CrossRef]
19. Pippan, R.; Hohenwarter, A. High pressure torsion (HPT). In *Severe Plastic Deformation Technology*; Rosochowski, A., Ed.; Whittles Publishing: Dunbeath, UK, 2017; p. 273, ISBN 978-1498784283.
20. Edalati, K.; Horita, Z.; Langdon, T.G. The significance of slippage in processing by high-pressure torsion. *Scr. Mater.* **2009**, *60*, 9–12. [CrossRef]
21. Kuhlmann-Wilsdorf, D.; Cai, B.C.; Nelson, R.B. Plastic flow between Bridgman anvils under high pressures. *J. Mater. Res.* **1991**, *6*, 2547–2564. [CrossRef]
22. Adachi, N.; Todaka, Y.; Yokoyama, Y.; Umemoto, M. Cause of hardening and softening in the bulk glassy alloy $Zr_{50}Cu_{40}Al_{10}$ after high-pressure torsion. *Mater. Sci. Eng. A* **2015**, *627*, 171–181. [CrossRef]
23. Dmowski, W.; Yokoyama, Y.; Chuang, A.; Ren, Y.; Umemoto, M.; Tsuchiya, K.; Inoue, A.; Egami, T. Structural rejuvenation in a bulk metallic glass induced by severe plastic deformation. *Acta Mater.* **2010**, *58*, 429–438. [CrossRef]
24. Gunderov, D.V.; Churakova, A.A.; Boltynjuk, E.V.; Ubyivovk, E.V.; Astanin, V.V.; Asfandiyarov, R.N.; Valiev, R.Z.; Xioang, W.; Wang, J.T. Observation of shear bands in the Vitreloy metallic glass subjected to HPT processing. *J. Alloys Compd.* **2019**, *800*, 58–63. [CrossRef]
25. Gunderov, D.V.; Astanin, V.V.; Sharafutdinov, A.V.; Bhatt, J. Slippage during high-pressure torsion processing of Vitreloy 105 bulk metallic glass. *J. Phys. Conf. Ser.* **2021**, *1967*, 012062. [CrossRef]
26. Gunderov, D.; Stotskiy, A.; Lebedev, Y.; Mukaeva, V. Influence of HPT and Accumulative High-Pressure Torsion on the Structure and Hv of a Zirconium Alloy. *Metals* **2021**, *11*, 573. [CrossRef]
27. Gunderov, D.; Asfandiyarov, R.; Raab, G.; Churakova, A.; Astanin, V. Method for slippage evaluation at various stages of high-pressure torsion and its application to Fe-0.1%C. *Lett. Mater.* **2021**, *11*, 416–421. [CrossRef]
28. Gunderov, D.; Asfandiyarov, R.; Titov, V.; Gunderova, S.; Astanin, V. Some Slippage Issues in High-Pressure Torsion Using Cu and Ti Samples as an Example. *Materials* **2022**, *16*, 162. [CrossRef]
29. Valiev, R. Nanostructuring of metals by severe plastic deformation for advanced properties. *Nat. Mater.* **2004**, *3*, 511–516. [CrossRef] [PubMed]
30. Karavaeva, M.V.; Nurieva, S.K.; Zaripov, N.G.; Ganeev, A.V.; Valiev, R.Z. Microstructure and mechanical properties of medium-carbon steel subjected to severe plastic deformation. *Met. Sci. Heat Treat.* **2012**, *54*, 155–159. [CrossRef]
31. Dobatkin, S.V.; Odessky, P.D.; Shagalina, S.V. Ultrafine Grained Low Carbon Steels Processed by Severe Plastic Deformation. *Mater. Sci. Forum* **2008**, *584–586*, 623–630. [CrossRef]
32. Straumal, B.B.; Gornakova, A.S.; Mazilkin, A.A.; Fabrichnaya, O.B.; Kriegel, M.J.; Baretzky, B.; Jiang, J.-Z.; Dobatkin, S.V. Phase transformations in the severely plastically deformed Zr–Nb alloys. *Mater. Lett.* **2012**, *81*, 225–228. [CrossRef]
33. Rogachev, S.O.; Nikulin, S.A.; Rozhnov, A.B.; Gorshenkov, M.V. Microstructure, Phase Composition, and Thermal Stability of Two Zirconium Alloys Subjected to High-Pressure Torsion at Different Temperatures. *Adv. Eng. Mater.* **2018**, *20*, 1800151. [CrossRef]
34. Edalati, K.; Horita, Z.; Mine, Y. High-pressure torsion of hafnium. *Mater. Sci. Eng. A* **2010**, *527*, 2136–2141. [CrossRef]
35. Zhilyaev, A.P.; Sharafutdinov, A.V.; Pérez-Prado, M.T. Phase Transformations During High-Pressure Torsion of Pure Zr and of a Zr-2.5%Nb Alloy. *Adv. Eng. Mater.* **2010**, *12*, 754–757. [CrossRef]
36. Tavares, S.S.M.; Gunderov, D.; Stolyarov, V.; Neto, J.M. Phase transformation induced by severe plastic deformation in the AISI 304L stainless steel. *Mater. Sci. Eng. A* **2003**, *358*, 32–36. [CrossRef]
37. Litovchenko, I.; Tyumentsev, A.; Korznikov, A.V. Reversible Martensitic Transformation Produced by Severe Plastic Deformation of Metastable Austenitic Steel. *Mater. Sci. Forum* **2013**, *738–739*, 491–495. [CrossRef]
38. Kozhevnikova, I.A. On the question of contact friction during rolling. *Bull. Cherepovetsky State Univ.* **2011**, *4–3*, 18–21.
39. Stembalski, M.; Preś, P.; Skoczyński, W. Determination of the friction coefficient as a function of sliding speed and normal pressure for steel C45 and steel 40HM. *Arch. Civ. Mech. Eng.* **2013**, *13*, 444–448. [CrossRef]

40. Gunderov, D.; Astanin, V. Influence of HPT Deformation on the Structure and Properties of Amorphous Alloys. *Metals* **2020**, *10*, 415. [CrossRef]
41. Beygelzimer, Y.; Estrin, Y.; Kulagin, R. Some Unresolved Problems of High-Pressure Torsion. *Mater. Trans.* **2023**, MT-MF2022038. [CrossRef]
42. Gunderov, D.V.; Churakova, A.A.; Astanin, V.V.; Asfandiyarov, R.N.; Hahn, H.; Valiev, R.Z. Accumulative HPT of Zr-based bulk metallic glasses. *Mater. Lett.* **2020**, *261*, 127000. [CrossRef]
43. Gunderov, D.; Astanin, V.; Churakova, A.; Sitdikov, V.; Ubyivovk, E.; Islamov, A.; Wang, J.T. Influence of High-Pressure Torsion and Accumulative High-Pressure Torsion on Microstructure and Properties of Zr-Based Bulk Metallic Glass Vit105. *Metals* **2020**, *10*, 1433. [CrossRef]
44. Ramazanov, I.A.; Gunderov, D.V.; Astanin, V.V.; Sitdikov, V.D.; Zakiryanova, G.T.; Sharafutdinov, A. V Effect of accumulative high-pressure torsion on the structure of steel 10. *IOP Conf. Ser. Mater. Sci. Eng.* **2020**, *1008*, 012027. [CrossRef]
45. Gunderov, D.; Prokoshkin, S.; Churakova, A.; Sheremetyev, V.; Ramazanov, I. Effect of HPT and accumulative HPT on structure formation and microhardness of the novel Ti18Zr15Nb alloy. *Mater. Lett.* **2021**, *283*, 128819. [CrossRef]
46. Saito, Y.; Utsunomiya, H.; Tsuji, N.; Sakai, T. Novel ultra-high straining process for bulk materials development of the accumulative roll-bonding (ARB) process. *Acta Mater.* **1999**, *47*, 579–583. [CrossRef]
47. Höppel, H.W.; Westermeyer, M.; Kümmel, F.; Göken, M. The role of interfaces on the deformation mechanisms in bimodal Al laminates produced by accumulative roll bonding. *Adv. Eng. Mater.* **2020**, *22*, 2000145. [CrossRef]
48. Tayyebi, M.; Adhami, M.; Karimi, A.; Rahmatabadi, D.; Alizadeh, M.; Hashemi, R. Effects of strain accumulation and annealing on interfacial microstructure and grain structure (Mg and Al_3Mg_2 layers) of Al/Cu/Mg multilayered composite fabricated by ARB process. *J. Mater. Res. Technol.* **2021**, *14*, 392–406. [CrossRef]
49. Gurau, G.; Gurau, C.; Fernandes, F.M.B.; Alexandru, P.; Sampath, V.; Marin, M.; Galbinasu, B.M. Structural Characteristics of Multilayered Ni-Ti Nanocomposite Fabricated by High Speed High Pressure Torsion (HSHPT). *Metals* **2020**, *10*, 1629. [CrossRef]
50. Bouaziz, O.; Kim, H.S.; Estrin, Y. Architecturing of Metal-Based Composites with Concurrent Nanostructuring: A New Paradigm of Materials Design. *Adv. Eng. Mater.* **2013**, *15*, 336–340. [CrossRef]
51. Han, J.-K.; Lee, H.-J.; Jang, J.; Kawasaki, M.; Langdon, T.G. Micro-mechanical and tribological properties of aluminum-magnesium nanocomposites processed by high-pressure torsion. *Mater. Sci. Eng. A* **2017**, *684*, 318–327. [CrossRef]
52. Han, J.; Han, D.K.; Liang, G.Y.; Jang, J.; Langdon, T.G.; Kawasaki, M. Direct Bonding of Aluminum–Copper Metals through High-Pressure Torsion Processing. *Adv. Eng. Mater.* **2018**, *20*, 1800642. [CrossRef]
53. Kawasaki, M.; Han, J.-K.; Lee, D.-H.; Jang, J.; Langdon, T.G. Fabrication of nanocomposites through diffusion bonding under high-pressure torsion. *J. Mater. Res.* **2018**, *33*, 2700–2710. [CrossRef]
54. Danilenko, V.N.; Kiekkuzhina, L.U.; Parkhimovich, N.Y.; Khafizova, E.D.; Gunderov, D.V. Cu-Al metal matrix composite fabricated by accumulative HPT. *Mater. Lett.* **2021**, *300*, 130240. [CrossRef]
55. Danilenko, V.N.; Korznikova, G.F.; Zhilyaev, A.P.; Sergeev, S.N.; Khalikova, G.R.; Khisamov, R.K.; Nazarov, K.S.; Kiekkuzhina, L.U.; Mulyukov, R.R. Effect of annealing on the structure and phase composition of Al-Cu laminated metal-matrix composites produced by shear deformation under pressure. *IOP Conf. Ser. Mater. Sci. Eng.* **2018**, *447*, 012021. [CrossRef]
56. Danilenko, V.N.; Sergeev, S.N.; Baimova, J.A.; Korznikova, G.F.; Nazarov, K.S.; Khisamov, R.K.; Glezer, A.M.; Mulyukov, R.R. An approach for fabrication of Al-Cu composite by high pressure torsion. *Mater. Lett.* **2019**, *236*, 51–55. [CrossRef]
57. Bazarnik, P.; Bartkowska, A.; Romelczyk-Baishya, B.; Adamczyk-Cieślak, B.; Dai, J.; Huang, Y.; Lewandowska, M.; Langdon, T.G. Superior strength of tri-layered Al–Cu–Al nano-composites processed by high-pressure torsion. *J. Alloys Compd.* **2020**, *846*, 156380. [CrossRef]
58. Kawasaki, M.; Ahn, B.; Lee, H.; Zhilyaev, A.P.; Langdon, T.G. Using high-pressure torsion to process an aluminum–magnesium nanocomposite through diffusion bonding. *J. Mater. Res.* **2016**, *31*, 88–99. [CrossRef]
59. Kulagin, R.; Beygelzimer, Y.; Ivanisenko, Y.; Mazilkin, A.; Straumal, B.; Hahn, H. Instabilities of interfaces between dissimilar metals induced by high pressure torsion. *Mater. Lett.* **2018**, *222*, 172–175. [CrossRef]